

# Deposition of Gold Nanoparticles on Silica Spheres: A Sonochemical Approach

V. G. Pol,<sup>†</sup> A. Gedanken,<sup>\*,†</sup> and J. Calderon-Moreno<sup>‡</sup>

Department of Chemistry, Bar-Ilan University, Ramat-Gan, 52900, Israel, and Materials and Structures Laboratory, Tokyo Institute of Technology, 4259, Nagatsuta, Midori-ku, 226-8503 Yokohama, Japan

Received October 14, 2002. Revised Manuscript Received December 16, 2002

Gold nanoparticles with an average size of  $\sim 5$  nm were deposited on the surface of preformed silica submicrospheres with the aid of power ultrasound. The sonochemical reduction was carried out by ultrasonic irradiation in an argon atmosphere at room temperature. Ultrasonic irradiation of a slurry of silica submicrospheres, chloroauric acid ( $\text{HAuCl}_4$ ), and ammonia in an aqueous medium for 45 min yielded a gold–silica nanocomposite. By controlling reaction conditions, we could achieve the deposition of metallic gold on the surface of the silica spheres. A unique crystallization process of the silica particles is observed. The crystallization process is assisted by the gold nanoparticles yielding the cristobalite phase of silica at a relatively low temperature. The resulting gold-deposited silica submicrosphere samples were characterized with XRD, EDAX, TEM, TGA, DSC, HR-SEM, and FT-IR, photoacoustic, and UV–visible spectroscopy.

## Introduction

The science and technology of nanomaterials has created great excitement and expectations in the past few years. By its very nature, the subject is of immense academic interest, having to do with very tiny objects in the nanometer regime (1–100 nm). There has already been much progress in the synthesis, assembly, and fabrication of nanophase materials such as nanocrystals, nanowires, nanotubes, nanorods, nanoribbons, nanoflasks, nanospheres, quantum dots, and nanocoating. Equally important are the potential applications of these materials in a wide variety of technologies.<sup>1</sup> Thus, a broad, new field is being developed that requires the cooperation of chemists, physicists, and engineers. Chemists are increasingly concerned with the synthesis, structure, enhanced properties,<sup>2</sup> and simulation of advanced or novel materials. The nanoparticles coated on a silica substrate provide a high surface area and possess chemical and physical properties that are distinct from those of both the bulk phase and individual molecules. They have the potential for application in optics, optoelectronics, catalysis, chemical engineering, pharmaceuticals, biology, and so forth. In view of the importance of the surface structure of nanoparticles on their properties, much effort has been invested in order to create new classes of materials through the modification of surface structure.<sup>3</sup>

Various groups have employed a range of wet-chemistry methods to modify or coat colloids with nanoparticles of noble metals. These include platinum nanoparticles coated on polystyrene microspheres.<sup>4</sup> Oldenburg et al. reported on a colloid reduction chemical route for the formation of solid-core/gold nanoshell particles.<sup>5</sup> The deposition of silver nanoparticles on silica spheres was carried out using an inverse micelle method,<sup>6</sup> nonionic reverse micelles,<sup>7</sup> pretreatment steps in electroless plating,<sup>8</sup> and the sol–gel method.<sup>9</sup> However, complicated apparatus, complex process control, and special conditions are required for these approaches.

In the present work, we describe an additional method, that is, an ultrasound-driven synthesis for coating nanosized gold particles on silica spheres. Sonochemistry is an alternative technique that can be employed for the production of coated particles. Power ultrasound effects chemical changes due to cavitation phenomena involving the formation, growth, and implosive collapse of bubbles in liquid.<sup>10a</sup> Sonication of the precursor in the presence of an inorganic support such as silica spheres provides an alternative means of trapping the nanometer clusters, which produce active supported heterogeneous catalysts. This phenomenon has been exploited to prepare a variety of metal nanoparticles and oxide nanorods<sup>10b</sup> and has recently been extended to produce core–shell-type materials.<sup>10c</sup> This

\* Corresponding author. Fax: +972-3-5351250. E-mail: gedanken@mail.biu.ac.il.

<sup>†</sup> Bar-Ilan University.

<sup>‡</sup> Tokyo Institute of Technology.

(1) Rao, C. N. R.; Cheetham, A. K. *J. Mater. Chem.* **2001**, *11*, 2887.  
(2) Mann, S.; Archibald, D. D.; Didymus, J.; Douglas, M. T.; Heywood, B. R.; Meldrum, F. C.; Reeves, M. J. *Science* **1993**, *261*, 1.  
(3) Fendler, J. H. *Nanoparticles and Nanostructured Films: Preparation, Characterization and Applications*; John Wiley & Son Ltd.: New York, 1998.

(4) Chen, C. W.; Serizawa, T.; Akashi, M. *Chem. Mater.* **1999**, *11*, 1381.

(5) Oldenburg, S. J.; Averitt, R. D.; Wetcott, S. L.; Halas, N. J. *Chem. Phys. Lett.* **1998**, *288*, 243.

(6) Ianos, P.; Thomas, J. K. *J. Colloid Interface Sci.* **1987**, *117*, 505.

(7) Zhang, Z. B.; Cheng, H. M.; Ma, J. M. *J. Mater. Sci. Lett.* **2001**, *20*, 439.

(8) Kobayashi, Y.; Salgueirino-Maceiraa, V.; Liz-Marzan, L. M. *Chem. Mater.* **2001**, *13*, 1630.

(9) Shibata, S.; Aoki, K.; Yano, T.; Yamane, M. *J. Sol.-Gel Sci. Technol.* **1998**, *11*, 279.

method has previously been used to disperse gold nanoparticles within the pores of mesoporous silica.<sup>10d</sup> In one of our recent publications we report that we have uniformly deposited metallic silver<sup>10e</sup> nanoparticles on silica spheres by controlling experimental conditions, and the submicrometer-size particles of titania were also coated by a nanolayer of europium oxide<sup>10f</sup> with the aid of power ultrasound, in a similar way, CdS<sup>10g</sup> and Eu<sub>2</sub>O<sub>3</sub><sup>10h</sup> also coated on silica spheres. Ultrasound-induced cavitation has also been used to coat nanosized nickel on alumina microspheres,<sup>10i</sup> and iron/iron oxide on silica spheres,<sup>10j</sup> imparting a magnetic function to the particles.

The use of spherical colloid particles as supports for the deposition of smaller noble metal particles has become appealing, as it permits the construction of novel colloids. The silica spheres used in our experiment as the substrate for gold deposition were made by modifying the Stöber<sup>11a</sup> method. The silica spheres qualify as hard spherical substrates for the following reasons: (a) narrow size distribution can be achieved over a wider range; (b) their surface silanol composition and the extent of hydrogen bonding can be modified by thermal treatment to change their reactivity; (c) silanol groups can form covalent links; and (d) the isotropic interactions in an aqueous or organic suspension help to form ordered arrays on substrates. In this report, we present results related to the sonochemical deposition of gold nanoparticles on spherical silica of various sizes. The resulting gold-deposited silica submicrosphere samples were characterized by X-ray diffraction, energy-dispersive X-ray analysis, transmission electron microscopy, high-resolution scanning electron microscopy, thermogravimetric analysis, differential scanning calorimetry, and Fourier transform infrared, photoacoustic, and UV-visible spectroscopy. In addition, a unique crystallization process of the silica particles, assisted by the gold nanoparticles yielding the cristobalite phase of silica at a relatively low temperature, is discussed.

## Experimental Section

**1. Preparation of Substrate.** Tetraethyl orthosilicate was purchased from Aldrich and used without further purification. Amorphous submicrospheres of silica in the various sizes were synthesized by base-catalyzed hydrolysis of TEOS. Initially, silica spheres were made by base-catalyzed hydrolysis of tetraethyl orthosilicate (TEOS) by the Stöber<sup>11a</sup> method. It is possible to synthesize monodispersed silica spheres in the 200–600-nm range by using this method. It becomes important to modify this method to synthesize monodispersed silica spheres from 100 to 1000 nm. The modification of the Stöber

**Table 1. Amount of the Reactants Used for the Preparation of Samples and TEM and EDAX Results**

sample no. <sup>a</sup>	silica used	gold precursor	coating thickness	Au analysis by EDAX
1	200 mg (800 nm)	0.2 mL	~4 nm	6.2 wt %
2h	200 mg (500 nm)	0.25 mL	~4 nm	7.3 wt %
3h	200 mg (500 nm)	0.35 mL	4–6 nm	9.9 wt %
4h	200 mg (500 nm)	0.45 mL	6–8 nm	11.8 wt %

<sup>a</sup> h = sample heated at 500 °C for 3 h.

process is explained briefly as follows. Considering that the ammonia is an essential component for the formation of spherical SiO<sub>2</sub> particles, instead of adding ammonia and ethanol separately, we used an ammonia-saturated ethanol (ASE) solution. Ammonium hydroxide was heated in a conical flask at 44–45 °C and released gaseous ammonia. This ammonia gas was bubbled into ethanol for 1 h to prepare an ASE solution (pH = 8.5–9). For each experiment, a fixed amount of ASE and distilled water was mixed in an Erlenmeyer flask and closed with a rubber seal. The optimized amount of TEOS was then injected quickly. The added amount of TEOS (3–7 mL) also affected the particle size uniformity. An increase in TEOS amount increases the particle diameter during seed growth. This mixture was stirred with a magnetic stirrer with a maximum mixing speed for 3 h. All the reactions were carried out with a total reaction volume of 100 mL.

Our approach was to maintain constant volumes, concentrations of water, and ASE for all reactions to achieve the monodispersity of the silica spheres. By maintaining constant volumes, concentrations of solvents, and the seed growth method, we could prepare monodispersed silica spheres up to a diameter of 1000 nm (unpublished). Silica submicrospheres thus obtained were washed extensively with ethanol in a centrifuge (8000 rpm) and dried under vacuum at room temperature for 8 h. The silica submicrospheres were heated at 500 °C for 3 h prior to their use in the sonochemical reaction, to remove surface OH groups, thus preventing coagulation of the spheres.<sup>10g</sup> In the present research work, we used annealed silica submicrospheres of 500- and 800-nm diameter.

**2. Sonochemical Deposition of Gold Nanoparticles.** Chloroauric acid (HAuCl<sub>4</sub>) was purchased from Aldrich and used without further purification. A microliter-size syringe (Hamilton Co.) was used to measure an accurate amount of chloroauric acid. Doubly distilled water was used for the sonication. The annealed silica submicrospheres (200 mg) and 0.2 mL of chloroauric acid were added to 100 mL of distilled water in a sonication cell, and the cell was attached to the sonicator horn under flowing argon. Argon gas was bubbled through the slurry for 2 h prior to sonication to expel dissolved oxygen/air. The sonication of the slurry with the high-intensity ultrasound radiation was carried out for 45 min by direct immersion of the titanium horn (Sonics and Materials VCX600 sonifier, 20 kHz, 40 W/cm<sup>2</sup>) in a sonication cell. A 5–7-mL portion of 24 wt % aqueous ammonia was added in drops during the sonication. A sonication cell was placed in an acetone-cooling bath, with a temperature of 20–25 °C maintained during the sonication. The product was washed thoroughly (twice) with doubly distilled deoxygenated water and centrifuged at 9000 rpm. The product was then dried in a vacuum for 12 h. The vacuum-dried product is termed the “as-prepared” sample. We also carried out a control reaction without the addition of ammonia, while maintaining all other conditions as before. Crystallization of the as-prepared product was carried out by heating a small amount of the sample in a boat crucible at a temperature of 500 °C for 3 h. The amount of the reactants for the preparation of samples and TEM and EDAX results are presented in Table 1.

**3. Characterization.** The X-ray diffraction patterns of the product were measured with a Bruker AXS D\* Advance Powder X-ray diffractometer (using Cu Kα = 1.5418 radiation). The elemental composition of the material was analyzed by energy-dispersive X-ray analysis (JEOL-JSM 840 scanning electron microscope). The particle morphology and the nature of the gold nanoparticles' adherence to silica spheres were

(10) (a) *Ultrasound: Its Chemical, Physical and Biological Effects*, Suslick, K. S., Ed.; VCH: Germany, 1988. (b) Pol, V. G.; Palchik, O.; Gedanken, A.; Felner, I. *J. Phys. Chem. B* **2002**, *106*, 9737. (c) Dokoutchaev, A.; James, J. T.; Koene, S. C.; Pathak, S.; Prakash, G. K. S.; Thompson, M. E. *Chem. Mater.* **1999**, *11*, 2389. (d) Chen, W.; Cai, W. P.; Liang, C. H.; Zhang, L. D. *Mater. Res. Bull.* **2001**, *136*, 335. (e) Pol, V. G.; Srivastava, D. N.; Palchik, O.; Palchik, V.; Slifkin, M. A.; Weiss, A. M.; Gedanken, A. *Langmuir* **2002**, *18*, 3352. (f) Pol, V. G.; Reisfeld, R.; Gedanken, A. *Chem. Mater.* **2002**, *14*, 3920. (g) Das, N. A.; Zaban, A.; Gedanken, A. *Chem. Mater.* **1999**, *11*, 806. Dhas, N. A.; Gedanken, A. *Appl. Phys. Lett.* **1998**, *72*, 2514. (h) Ramesh, S.; Minti, H.; Reisfeld, R.; Gedanken, A. *Opt. Mater.* **1999**, *13*, 67. (i) Zhong, Z.; Mastai, Y.; Koltipin, Y.; Zhao, Y.; Gedanken, A. *Chem. Mater.* **1999**, *11*, 2350. (j) Ramesh, S.; Prozorov, R.; Gedanken, A. *Chem. Mater.* **1997**, *9*, 2996.

(11) (a) Stöber, W.; Fink, A.; Bohn, E. *J. Colloid Interface Sci.* **1968**, *26*, 62. (b) Slifkin, M. A.; Luria, L.; Weiss, A. M. *Proc. SPIE-Int. Soc. Opt. Eng.* **1998**, *3110*, 481.

studied with transmission electron microscopy, which was done on a JEOL-JEM 100 SX microscope, working at a 100-kV accelerating voltage. A small quantity of sample was added in ethanol and sonicated for 20 min in a vial by using a sonication bath. One or two drops of the nanoparticle solution were deposited on a copper grid. With the grid kept on Whatmann filter paper, it absorbed the droplet and dried the excess solvent in 5–10 min. High-resolution scanning electron microscope (HR-SEM) images were obtained using an LEO Gemini 982 field emission gun SEM (FEG-SEM) operating at 4-kV accelerating voltage. The sample was placed and pressed on double-sided conducting carbon tape supported by a copper plate. The excess sample was removed by spraying air on the sample holder. Silica submicrosphere surfaces were imaged using standard instrumentation and conditions, with the exception that samples were not sputter-coated with gold prior to imaging. Thermogravimetric analysis of the as-prepared sample was carried out under a stream of nitrogen, at a heating rate of 3 °C/min using a Mettler TGA/STDA 851. Differential scanning calorimetric (DSC) analysis of the as-prepared sample in a crimped aluminum crucible was carried out up to a temperature of 500 °C, using a Mettler DSC-301 under a stream of nitrogen, at a heating rate of 3 °C/min. Fourier transform infrared spectroscopy was carried out on a Nicolet Impact 410 FTIR spectrometer. Fourier transform infrared (FT-IR) studies were taken into consideration in this research work for the analysis of the various reactive species on the surface of silica, and for the assessment of the extent of interaction between the metal and the silica surface. The pellets of KBr were measured by keeping the ratio of nanoparticles to KBr at 1:25. Absorption spectroscopy was carried out at room temperature on a LKB Biochem (Ultraspec II 4050 UV–visible spectrophotometer) over the wavelength region of 400–700 nm. A small quantity of the sample was added in distilled water, sonicated for 20 min in a vial using a sonication bath for dispersion, and loaded into a quartz cell for analysis. Photoacoustic spectroscopy measurements were conducted by employing a homemade instrument based on one which was described elsewhere,<sup>11b</sup> but with completely updated software.

### Proposed Sonochemical Mechanism for the Deposition of Gold Nanoparticles on Silica Submicrospheres

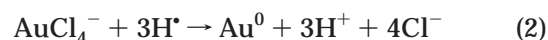
The chemical reactions can be driven by intense ultrasonic waves, which are strong enough to produce oxidation, reduction, dissolution, and decomposition.<sup>12–14</sup> Three different regions are formed<sup>15</sup> during an aqueous sonochemical process: (a) the inner environment (gas phase) of the collapsing bubbles, where elevated temperatures (several thousand degrees) and pressure (hundreds of atmospheres) are produced, causing water to pyrolyze into H and OH radicals; (b) the interfacial region where the temperature is lower than that in the gas-phase region, but still high enough to induce a sonochemical reaction (a few hundred degrees Celsius); and (c) the bulk solution, which is at ambient temperature. The present reaction appears to occur within the interfacial region because it is clear that AuCl<sub>4</sub><sup>−</sup> ions cannot be found inside the collapsing bubble (in the gas phase).

To establish the mechanism of this reaction, a number of control experiments were conducted. In a control

reaction, silica, HAuCl<sub>4</sub>, and NH<sub>3</sub> in the same ratio were vigorously stirred in an aqueous solution, without sonication, and no gold nanoparticles were obtained. A second control experiment was carried out with the same reagents, without sonication but with regular heating (refluxing for a few hours). In this case, a few gold particles were obtained, but the silica spheres remained uncoated, thus showing that temperatures higher than 100 °C are required for the rupture of the Si–O–Si bonds. The temperatures, which are attributed to the inner environment of the bubble or interfacial region,<sup>15</sup> are in fact much higher than 100 °C. We are therefore led to assume that the formation of the Au nanoparticles occurs in the interfacial region. The low abundance of gold ions in the ~200-nm bubble ring (this is the approximate size of the interfacial region)<sup>15</sup> is the reason for the formation of nanoparticles. This mechanism of the formation of Au nanoparticles takes into consideration the fact that free radical species are generated from water molecules by the absorption of ultrasound (eq 1). This would be the initiation reaction.



The H radical formed in eq 1 can act as a reducing species and trigger the reduction (eq 2).



The sonochemical reduction process generates high temperatures and pressures for the reduction of HAuCl<sub>4</sub> to amorphous gold. In the sonochemical formation of gold nanoparticles in an aqueous solution, Nagata et al. studied the rate of formation and stability of gold nanoparticles<sup>16</sup> in a variety of surfactants (PEG 40, SDS, PVP, ethanol, etc.) They also proposed that the hydrogen atoms formed are consumed via recombination of Au(III) to Au(0) in sonolysis of pure water.

Ammonia also plays an important role in the current process. On the basis of our control experiment where a poor coating was achieved in the absence of ammonia, we correlate that ammonia can activate the SiO<sub>2</sub> surface to produce reactive silanol groups. An additional control reaction was carried out with vigorous mixing, but without sonication. It yielded only micrometer-sized gold particles, and no coating of the silica spheres was detected. The mechanism by which the gold nanoparticles are bonded to the silica surface is related to the microjets and shock waves created near solid surfaces after the collapse of the bubble.<sup>17</sup> These jets, which cause, for example, the sintering of micrometer-sized metallic particles,<sup>17</sup> push the nanoparticles toward the silica surface at very high speeds. When they hit the silica surface, they can react with free silanols, or even Si–O–Si bonds. This may result in the formation of Au–O–Si bonds, even when they were not formed on the SiO<sub>2</sub> surface.

## Results and Discussion

**1. X-ray Diffraction (XRD) and Energy-Dispersive X-ray Analysis (EDAX).** In Figure 1a, we present

(12) Suslick, K. S.; Choe, S. B.; Cichowlas, A. A.; Grinstaff, M. W. *Nature* **1991**, *353*, 414.

(13) Gutierrez, M.; Henglein, A.; Dohrmann, J. *J. Phys. Chem.* **1987**, *91*, 6687.

(14) Alegria, A. E.; Lion, Y.; Kondo, T.; Riesz, P. *J. Phys. Chem.* **1989**, *93*, 4908.

(15) Suslick, K. S.; Hammerton, D. A. *IEEE Trans. Sonics Ultrason.* **1986**, *SU-33*, 143.

(16) Nagata, Y.; Mizukoshi, Y.; Okitsu, K.; Maeda, Y. *Radiat. Res.* **1996**, *146*, 333.

(17) Suslick, K. S.; Price, G. J. *Annu. Rev. Mater. Sci.* **1999**, *29*, 295.



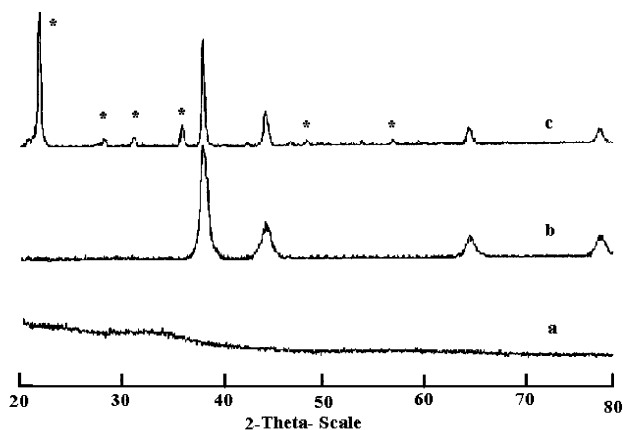


**Figure 1.** X-ray diffraction patterns of (a) sample 2, (b) sample 2h, and (c) sample 2 after TGA measurement (\* indicates the peaks of cristoballite phase of silica).

the X-ray diffraction pattern of the as-prepared gold-coated silica submicrosphere sample. The amorphous nature of the product is demonstrated by the absence of any diffraction peaks. The XRD pattern for the heated sample (500 °C/3 h) is shown in Figure 1b. It shows the formation of a face-centered cubic phase of metallic gold (PDF: 4-784). The peaks at  $2\theta = 38.18^\circ$ ,  $44.39^\circ$ ,  $64.58^\circ$ , and  $77.54^\circ$  are assigned as (111), (200), (220), and (311) reflection lines, respectively, of fcc Au particles. No peak characteristic of any impurities were observed.

Surprisingly, it was observed that sample 2, annealed during thermogravimetric analysis up to 1000 °C under a flowing stream of nitrogen, at a heating rate of 3 °C/min shows two phases in XRD measurement. These are the fcc Au (PDF: 4-784) and tetragonal cristobalite (silicon dioxide, PDF: 39-1425). The crystallization temperature of amorphous silica forming the crystalline phase was reported<sup>18a</sup> as 1300 °C. To check whether the low-temperature crystallization is due to a size effect or to induced crystallization due to the gold nanoparticles, bare silica spheres were annealed at 1000 °C in a furnace under flowing nitrogen gas. XRD measurements confirmed that the silica heated to 1000 °C is amorphous in nature, contrary to the annealed sample 2, which shows the two phases, namely, fcc Au and tetragonal cristobalite. This means that coated gold nanoparticles induce silica crystallization at a lower temperature. The presence of metal disrupts the amorphous network, reducing the kinetic barrier to the crystallization.

To discover the exact crystallization temperature of silica, we annealed the gold-coated silica spheres at 600, 700, 800, 850, 900, and 950 °C. The samples annealed at 600, 700, and 800 °C were featureless. The 100% intense diffraction peak corresponds to the silica [101] plane over the  $2\theta$  range of 20–25°. The diffraction patterns were scanned only in this region. XRD patterns from Au-coated silica submicrosphere samples annealed in nitrogen at 800, 850, 900, and 950 °C are shown in a, b, c, and d, respectively, of Figure 2. The increase in the peak intensity corresponds to the [101] plane observed with an increase in the temperature. It depicts

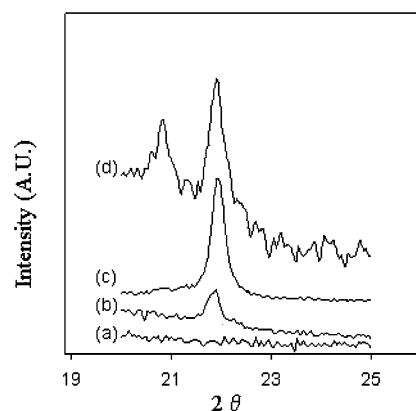


**Figure 2.** X-ray diffraction patterns of sample 2 annealed at (a) 800 °C, (b) 850 °C, (c) 900 °C, and (d) 950 °C.

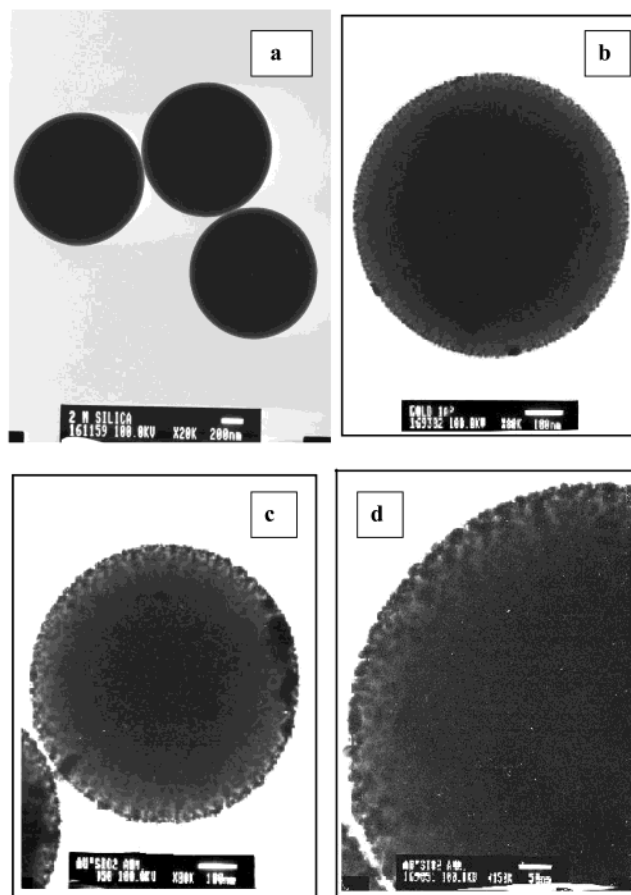


**Figure 3.** Transmission electron micrographs of (a) the bare substrate silica submicrospheres (800 nm), (b) as-prepared sample of a gold-deposited silica submicrosphere, (c) crystalline gold nanoparticles deposited on silica submicrospheres, and (d) an Au-coated silica submicrosphere shown at high resolution.

that, at 950 °C, all amorphous silica transformed into cristobalite.

According to our experimental results, thermal treatments at low temperature promote crystallization of amorphous  $\text{SiO}_2$  into the cristobalite phase only when the surface is coated with gold. A similar effect of considerable lowering of amorphous-to-crystalline transition temperature was observed for amorphous  $\text{SiO}_2$  and silver<sup>18b</sup> (~800 °C). Garnica-Romo and co-workers<sup>18b</sup> proposed that the mentioned effect could be the influence of the metal–glass interface. The increase in the

(18) (a) Sneh, O.; George, S. *J. Phys. Chem.* **1995**, *99*, 4639. (b) Garnica-Romo, M. G.; Gonzalez-Hernandez, J.; Hernandez-Landaverde, M. A.; Vorobiev, Y. V.; Ruiz, F.; Martinez, J. R. *J. Mater. Res.* **2001**, *16*, 2007.

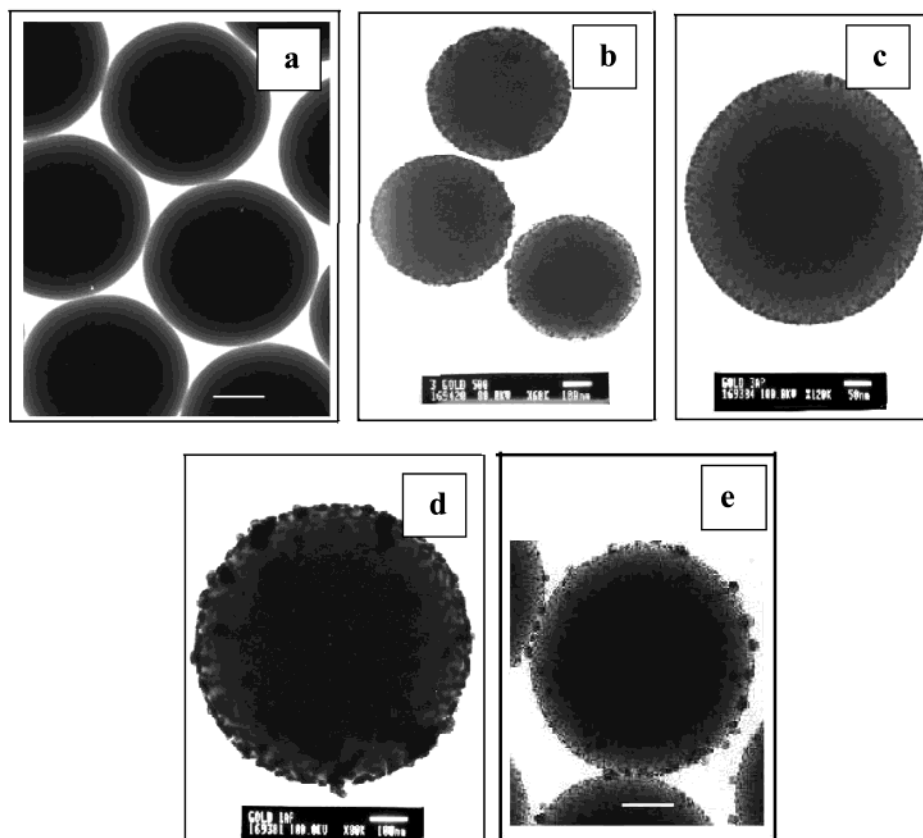


**Figure 4.** Transmission electron micrographs of (a) bare substrate silica submicrospheres (500 nm) (bar indicates 130 nm), (b) sample 2h, (c) sample 3h, (d) sample 4h, and (e) different sizes of crystalline gold nanoparticles deposited on silica submicrospheres (bar indicates 100 nm).

amplitude in the ionic vibrations in the glass near the metal surface is due to the electrostatic screening of the ion's charge by the metal. The result could be viewed as local heating, where the local atomic ordering is already close to the structure of cristobalite so that only a small atomic-bonding rearrangement is necessary for crystallization.

The presence of gold, silicon, and oxygen in the coated materials was examined with EDAX measurements. The EDAX spectrum was also used to obtain a quantitative estimate of the Au and Au/Si ratios. For the light elements such as oxygen, only a rough estimate could be made. Therefore, the Au/O ratio is not an accurate estimate. The gold content in samples 1 and 2 were about 6 and 7 wt %, respectively. While samples 3 and 4 show around 10 and 12 wt % gold content, respectively, the gold, silicon, and Au/Si ratio in samples 1h, 2h, 3h, and 4h were identical with respect to the as-prepared samples. These values are close to the molar ratio of  $\text{HAuCl}_4/\text{SiO}_2$  in the starting solution.

**2. Electron Microscopy Studies (TEM and HR-SEM).** TEM and high-resolution SEM were used to study the gold-coated nanoparticles' morphology and the nature of its adherence to the silica spheres. In our first set of experiments, we optimized the amount of gold precursor for 200-mg (800 nm) silica spheres coating. Figure 3a shows the transmission electron micrographs of preformed submicrospherical silica particle substrates, which were used in this study. The TEM micrograph of the silica spheres deposited with amorphous gold nanoparticles is shown in Figure 3b. In this

case, the silica spheres were coated with a uniform amorphous layer. In the case of the heated sample 1 (500 °C/3 h), all of the silica submicrosphere surfaces are almost uniformly covered with gold nanosized particles (Figure 3c). In Figure 3d, a submicrosphere of silica deposited with crystalline gold nanoparticles is shown at a higher resolution. More than 95% of the coated gold nanoparticles have a diameter of approximately 5 nm uniformly covering the surface of the silica submicrospheres.

In our second set of experiments, we have coated 500-nm silica spheres (200 mg) with various concentrations of the gold precursor. We varied gold precursor concentration from 0.25 to 0.55 mL to check the coating nature. It was confirmed from the first set of experiments that a minimum of 0.2 mL of Au precursor would be necessary to coat 800-nm (200 mg) silica spheres. We observed that a 0.25-mL Au precursor is required to coat uniformly silica spheres of 500-nm diameter (200 mg). The TEM micrograph of 500-nm uncoated silica spheres (Figure 4a) shows that they are smooth and monodispersed prior to gold nanoparticle coating. The silica spheres were coated with a uniform layer of 3–4-nm gold nanoparticles (sample 2h, Figure 4b). In another experiment, we have increased the amount of gold precursor to 0.35 mL in an attempt to examine the role of excess gold. We have observed that under these coating conditions a thicker coating layer (~4–6 nm) was obtained (sample 3h, Figure 4c). Further successive deposition of a gold (0.45-mL precursor) nanoparticle results in an increase in the coated particle diameter

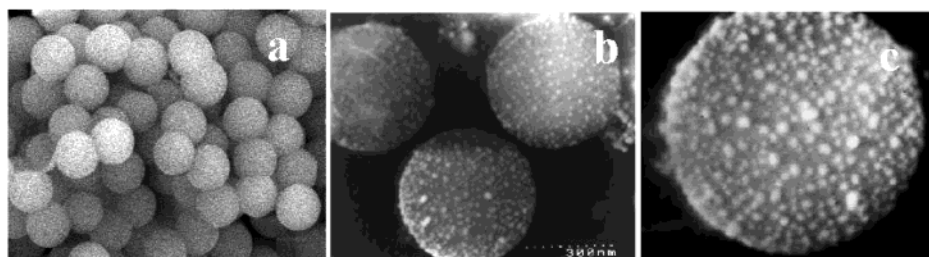


**Figure 5.** Scanning electron micrographs of (a) bare silica submicrospheres, (b) silica submicrospheres deposited with gold nanoparticles (sample 2h), and (c) silica submicrospheres deposited with gold nanoparticles (sample 2h) shown at higher resolution.

(sample 4, Figure 4d). Here, the gold-coated particle diameter was around 6–8 nm. The average incremental diameter increase for each successive addition of gold precursor is 2–3 nm. It is possible to coat uniformly gold particles on the silica surface up to the addition of 0.45 mL of gold precursor. When the amount of the gold precursor reached 0.55 mL, keeping other reaction conditions as in the previous experiments, two sizes of gold layers were observed, 2 and 8 nm. This means that during the sonochemical reaction two types of particles were formed and result in nonuniform coating (Figure 4e). Addition of more than 0.55 mL of gold precursor resulted in the same results in addition to free uncoated particles (~10 nm). These results show that optimization of the amount of gold precursor is equally important to other reaction conditions. Das et al. observed ZnS nanoparticles (1–5 nm in diameter) that covered the colloidal silica surface, either as a thin layer or as nanoclusters, depending on the reactant concentrations.<sup>10g</sup> Dokoutchaev et al. recently reported the alternating assembly of metal nanosized particles and oppositely charged polyelectrolyte onto polystyrene microspheres. In that work<sup>10c</sup> a low gold coverage and nonuniform coatings of nanoparticles were obtained, although the nanoparticle loading was increased by repeated depositions of nanoparticle and polyelectrolyte in the LBL (layer-by-layer) manner. For silica coatings, Caruso et al. reported that approximately one monolayer of nanoparticles was absorbed with each deposition step.<sup>19</sup> In our two sets of experiments, the TEM images illustrate nanoscale control, regularity, and uniformity of the coatings.

The HR-SEM micrograph of the monodispersed bare silica is shown in Figure 5a. Figure 5b,c (at high resolution) clearly shows the nanoparticles of Au coated on the spherical silica surface (sample 2h). These results are in good agreement with our TEM measurements.

**3. Photoacoustic Spectroscopy.** The results of the photoacoustic measurements are shown in Figure 6a,b. Photoacoustic spectroscopy is a very sensitive optical absorption spectrometry, which is superior to both transmission or reflectance spectrophotometry for the measurement of the electronic properties of highly absorbing and/or scattering samples, such as nanoparticles.<sup>20a,b</sup> For example, although the absorption spectrum of the unheated sample 2, when measured

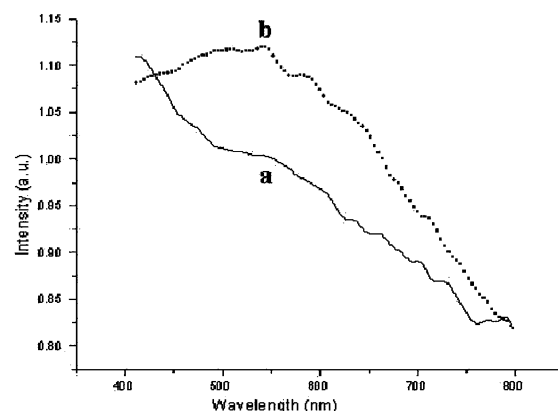


**Figure 6.** Photoacoustic spectra of (a) as-prepared Au coated on the silica submicrospheres (sample 2) and (b) sample 2 heated to 500 °C/3 h.

with a conventional spectrophotometer, was featureless (data not shown), the PA spectrum of the same sample showed a small, broad absorption signal in the range of 480–630 nm (Figure 6a). This absorption is most likely due to the semicrystalline nature of the as-deposited gold particles on the silica surface. These nanoparticles could not be detected by PXRD because of the limitation of the XRD method for measurements of very small nanoparticles. Such samples are known as “XRD-amorphous samples”.<sup>20c</sup> The ratio of this crystalline to amorphous gold was less, and in addition, the total quantity of gold in this sample was less than 7 at. %. When this sample was heated (to 500 °C), crystallization of the gold occurred, and a strong plasmon absorption band appeared on the PA spectrum at the same range. The maximum of this peak appeared at 542 nm, which is close to the result of absorption measurements of crystalline gold nanoparticles (see Figure 7c). Additional peaks were observed in the PA spectra at 508 and 586 nm. These peaks may be due to the size distribution of the crystalline-coated particles in the sample 2h.

**4. UV–Visible Absorption Measurements.** The optical absorption spectrum for the reference (preformed silica host) is shown in Figure 7a. The UV–visible absorption spectrum of annealed Au-coated silica spheres (sample 2h) is shown in Figure 7c. The figure demonstrates the formation of gold nanoparticles, in agreement with the XRD measurements. These nanoparticles exhibit an intense, broad absorption peak around 535 nm due to surface plasmon excitation. Surface plasmon excitation is a phenomenon that exists most commonly at the interface between a metal and a dielectric

(19) Caruso, F.; Lichtenfeld, H.; Mohwald, H.; Giersig, M. *J. Am. Chem. Soc.* **1998**, *120*, 8523.

(20) (a) Rosenzweig, A. *Photoacoustics and photoacoustic spectroscopy*; Academic Press: New York, 1980. (b) Palchik, O.; Kerner, R.; Gedanken, A.; Weiss, A. M.; Slifkin, M. A.; Palchik, V. *J. Mater. Chem.* **2001**, *11*, 874. (c) Bish, D. L.; Post, J. E. *Modern Powder Diffraction*; The Mineralogical Society of America: Washington, D.C., 1989.



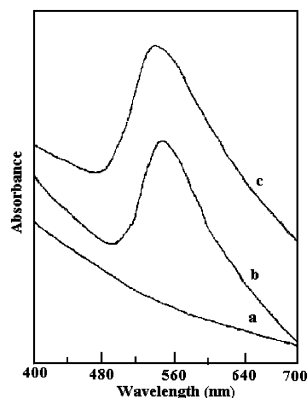


**Figure 7.** Absorption spectra of an aqueous solution containing (a) bare silica spheres, (b) crystalline Au nanoparticles deposited on silica submicrospheres (sample 4h), and (c) crystalline Au nanoparticles deposited on silica submicrospheres (sample 2h).

material, such as air and water.<sup>21</sup> Figure 7b depicts the spectrum of bigger size gold particles ( $\sim 8$  nm) coated on the surface of silica spheres (sample 4h). The spectrum is red-shifted and the broad absorption peak appears at 545 nm. Chen et al.,<sup>22a</sup> Kreibig and Vollmer,<sup>22b</sup> and Oldenberg et al.<sup>5</sup> reported that the peak position and width are dependent on the diameter of gold particles coated on the surface of silica spheres. Our spectra match well with their data. The full-width at half-maximum of this peak (spectrum 7b) is approximately equal to 80 nm, which corresponds to the 8-nm average diameter of the gold<sup>5</sup> nanoparticles. This is in agreement with our TEM measurements where 6–8-nm-coated particles could be detected from the TEM image.

**5. Thermal Properties.** The thermogravimetric analysis (TGA) curve of the gold-deposited silica spheres is shown in Figure 8a. The thermal analysis of this sample was carried out under a stream of nitrogen at a heating rate of 10 °C/min. The observed weight loss appeared in only one step. When the heating rate was reduced to 3 °C/min, a multistep weight loss is detected in the thermogravimetric analysis. The TGA pattern of the as-prepared product showed a total weight loss of 10% over the temperature ranges of 40–600 °C. The weight loss demands an understanding of the nature of thermally desorbed species on the surface of silica spheres. The surface of spherical silica consists of a very small portion of free silanols, a large amount of hydrogen-bonded silanols, and adsorbed water molecules.<sup>23,24a</sup> The hydrogen-bonded silanols show hydrogen bonding at the oxygen end, at the hydrogen end, and at both ends. These thermally removable species are present on the walls of the inner pores as well. The population of silanols and water molecules can be found on the outer spherical surface of the particles, as well as on the inner pore walls. The weight loss occurred in two distinct regions from 40 to 200 °C and from 350 to 560 °C. The

weight loss in the first step was 7.5%, whereas in the second step the weight loss was 2.5%. The first step weight loss in the temperature range of 40–200 °C can be associated with the breakup of the hydrogen-bonded network and the expulsion of adsorbed water from the surface. The second stage of weight loss, in the range of 350–560 °C, could be associated with desorption of the adsorbed water, as well as water generated by the condensation of part of free silanols on the inner pore walls. These results are in good agreement with the published article of Ramesh et al. They also observed a two-step weight loss process in cobalt nanoparticles<sup>24b</sup> coated on silica spheres. The end product of TGA measurements was found to be pure Au, and the cristobalite phase of silica as confirmed by powder XRD measurement.

The DSC curve (Figure 8b) for the as-prepared Au-deposited silica sample is shown. An exothermic peak was obtained at 165–220 °C with the maximum at 175 °C. To locate the amorphous-to-crystalline transition of gold nanoparticles coated on silica spheres, we annealed sample 2 at 250 °C, which is the highest temperature in this exothermic region. It was observed that the sample heated at 250 °C was well-crystallized, as confirmed by XRD measurements (same as Figure 1b). To explain the second exothermic peak at 375 °C, we carried out FT-IR measurements of the same sample at different temperatures. When the sample was cooled and reheated, the two exothermic peaks did not show up in the DSC spectrum (data not shown).

#### 6. Fourier Transform Infrared (FT-IR) Studies.

The FT-IR spectra of bare SiO<sub>2</sub> spheres, Au/SiO<sub>2</sub> annealed at 300 °C (sample 2), and Au-coated SiO<sub>2</sub> annealed at 450 °C (sample 2) are shown in Figure 9a–c. The IR spectrum after a thermal treatment at 300 °C shows one significant change, the disappearance of the 980-cm<sup>-1</sup> band, related to the stretching of isolated silanols and visible only in the bare silica spheres. Since the heating of the gold-coated spheres is not sufficient to condensate such silanols, the disappearance of the band can be considered as an indirect indication of gold bonding to the surface. The IR spectrum, after a thermal treatment at 450 °C, shows a significant increase in the intensity at the high-energy side of the stretching vibration of Si–O–Si bonds in the 1100–1250-cm<sup>-1</sup> range, and the associated broadening of the 1100-cm<sup>-1</sup> band (Figure 9c). The high intensity of the band is attributed to the breathing vibrations of a large population of rings formed by several Si–O–Si units.<sup>25,26</sup> The thermal treatment at 450 °C leads to the formation of stable siloxane rings in the amorphous matrix due to condensation reactions. It is interesting to note that, in the gold-coated silica spheres, the intensity of the high-energy band, and therefore the population of ordered rings, is significantly higher than that in bare silica spheres heated at 500 °C (Figure 9a). Although cristobalite is a high-temperature allotrope, its structure of six-membered rings is the most similar to amorphous silica; that is, it is the first crystalline phase to nucleate from the melt. A high population of ordered rings will favor the crystallization of the silica matrix into cris-

(21) *Optical effects associated with small particles*, Barber, P. W., Chang, R. K., Eds.; World Scientific: Singapore, 1988.

(22) (a) Chen, W.; Cai, W.; Wang, G.; Zhang, L. *Appl. Surf. Sci.* **2001**, 174, 51. (b) Kreibig, U.; Vollmer, M. *Optical properties of metal clusters*; Springer-Verlag: Berlin, 1995.

(23) Chuang, I.-S.; Maciel, G. E. *J. Am. Chem. Soc.* **1996**, 118, 401.

(24) (a) Tsuchiya, I. *J. Phys. Chem.* **1982**, 86, 4107. (b) Ramesh, S.; Cohen, Y.; Prossorov, R.; Shafi, K. V. P. M.; Aurbach, D.; Gedanken, A. *J. Phys. Chem. B* **1998**, 102, 10234.

(25) Galeener, F. L. *Phys. Rev.* **1979**, B15, 4292.

(26) Martinez, J. R.; Ruiz, F.; Vorobiev, Y. V.; Perez-Robles, F.; Gonzalez-Hernandez, J. *J. Chem. Phys.* **1998**, 109, 7511.

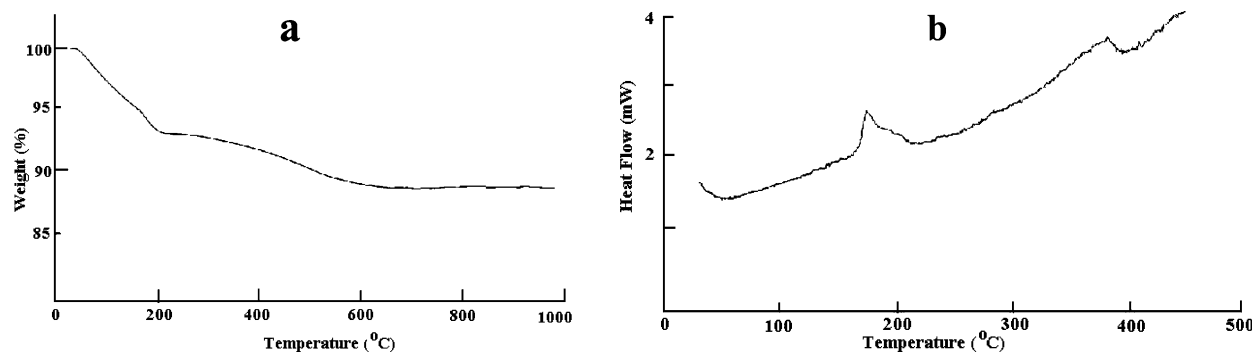


**Figure 8.** Thermogravimetric analysis (TGA) profile of (a) the as-prepared sample 2 of silica deposited with nanophasic amorphous gold and (b) DSC curve for sample 2.

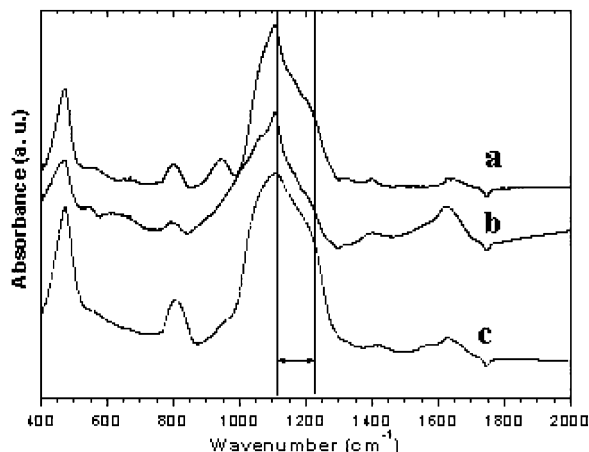


**Figure 9.** FT-IR spectra of (a) bare silica spheres, (b) Au coated on the silica submicrospheres (sample 2) heated at 300 °C/3 h, and (c) sample 2 heated to 450 °C/3 h. The changes in the region between  $\sim 1100$  and  $1200\text{ cm}^{-1}$ , marked with an arrow, indicate the formation of ordered rings in the silica matrix.

tobalite at lower temperatures.<sup>27</sup> The exothermic peak observed at  $\sim 375\text{ }^{\circ}\text{C}$  in the DSC measurements could be an indication of the formation of stable structures of several siloxane rings in the amorphous matrix. However, on the basis of the FT-IR spectra, it is not possible to determine the exact role of Au in promoting the crystallization of cristobalite at a low temperature. Some authors have proposed a catalytic effect of the metal, where enhanced thermal energy transfer from the metal clusters to the glass-silica network results in a local heating effect.<sup>28</sup> This catalytic effect has only been observed previously in the case of Ag.<sup>18b</sup> Au, in our present study, is the second example of this phenomenon. Other metals such as Fe, Co, and Cu do not exhibit this behavior. For Ag, a mechanism involving the formation of unstable oxidized metal species on the surface of the metal particles ( $\text{Ag}_2\text{O}$ ) has been suggested so that the thermal effect would be provided by the

decomposition of the unstable oxide, explaining why such a mechanism could not be active in the case of metal-forming stable oxides, such as Fe, Cu, or Co.<sup>29</sup> Further investigation into the interaction between metal nanoparticles and silica is currently underway and will be reported elsewhere.

### Conclusions

Gold nanoparticles of  $\sim 5\text{ nm}$  were deposited by ultrasound on the surface of silica submicrospheres. The presence of metallic gold on the silica support was evidenced by XRD, EDAX, photoacoustic, and UV-visible spectra. The morphology of the gold-coated particles and the nature of its adherence to silica spheres were studied with TEM and HR-SEM. FT-IR measurements were employed to explain the second exothermic peak at  $375\text{ }^{\circ}\text{C}$ , appearing in a DSC spectrum. The advantage of the process described in this report is that it is a simple, efficient, one-step synthesis that produces a uniform coating of gold nanoparticles on the silica submicrospheres. The period of sonication is only 45 min. Optimization of the amount of gold precursor required for the uniform deposition of gold nanoparticles on various sizes of silica surfaces was presented. We have also detected a unique crystallization process of the silica particles assisted by the gold nanoparticles yielding the cristobalite phase, at the Au/Silica interface, where crystallization probably starts due to a reduction in the kinetic energy for the crystallization.

**Acknowledgment.** V. G. Pol thanks Bar-Ilan University, Israel, for financial assistance through the President's Fund. The authors thank V. Palchik and A. M. Weiss for the photoacoustic measurements. A. Gedanken is grateful to the DIP Organization (Deutsche-Israeli Projects) for their financial help administered by the BHSF, Germany.

CM021013+

(27) Rino, J. P.; Ebbsjo, I.; Kalia, R. K.; Nakano, A.; Vashishta, P. *Phys. Rev.* **1993**, *B47*, 3053.

(28) Garcia-Rodriguez F. J. *J. Raman Spectrosc.* **1998**, *29*, 763.

(29) Altamirano-Juarez, D. C.; Carrera-Figueiras, C.; Garnica-Romo, M. G.; Mendoza-Lopez, M. L.; Ortuno-Lopez, M. B.; Perez-Ramos, M. E.; Ramos-Mendoza, A.; Rivera-Rodriguez, C.; Tototzintle-Huitle, H.; Valenzuela-Jauregi, J. J. *J. Phys. Chem. Solids* **2001**, *62*, 1911.